



ELSEVIER

journal homepage: www.elsevier.com/locate/epilepsires



A phantom and animal study of temperature changes during fMRI with intracerebral depth electrodes



Carolina Ciumas^{a,b,*}, Gregor Schaefers^c, Sandrine Bouvard^{a,b,d},
Emmeline Tailhades^e, Emmanuel Perrin^e,
Jean-Christophe Comte^b, Emmanuelle Canet-Soulas^f,
Chantal Bonnet^{a,b}, Danielle Ibarrola^d, Gustavo Polo^g,
Jose Moya^h, Olivier Beuf^e, Philippe Ryvlin^{a,b,d,i,**}

^a Translational and Integrative Group in Epilepsy Research (TIGER), INSERM, France

^b U1028, CNRS UMR 5292, Centre de Recherche en Neuroscience de Lyon, Lyon, France

^c MR:comp GmbH, Testing Services for MR Safety & Compatibility, Gelsenkirchen, Germany

^d CERMEP – Imagerie du Vivant, Lyon, France

^e CREATIS, CNRS UMR 5220, Inserm U1044, INSA-Lyon, Université Lyon 1, Villeurbanne, France

^f CarMeN, INSERM U1060, INSA de Lyon, Université de Lyon, Villeurbanne, France

^g Department of Functional Neurosurgery, Hospices Civils de Lyon, Lyon, France

^h DIXI, Besançon, France

ⁱ Department of Functional Neurology and Epileptology, Hospices Civils de Lyon, Lyon, France

Received 2 August 2013 ; received in revised form 2 October 2013; accepted 18 October 2013

Available online 28 October 2013

KEYWORDS

icEEG;
fMRI;

Summary

Background: MRI is routinely used in patients undergoing intracerebral electroencephalography (icEEG) in order to precisely locate the position of intracerebral electrodes. In contrast, fMRI has been considered unsafe due to suspected greater risk of radiofrequency-induced (RF) tissue heating at the vicinity of intracerebral electrodes. We determined the possible temperature change at the tip of such electrodes during fMRI sessions in phantom and animals.

Abbreviations: BOLD, bold oxygenation level dependency; icEEG, intracerebral electroencephalography; fMRI, functional magnetic resonance imaging; HFO, high frequency oscillation; ASTM, American Society of Testing and Materials; MRI, magnetic resonance imaging; RF, radiofrequency; MR, magnetic resonance; SAR, specific absorption rate; EPI, echo-planar imaging; FOV, field of view.

* Corresponding author at: TIGER, Translational and Integrative Group in Epilepsy Research, INSERM U1028, CNRS UMR 5292, Centre de Recherche en Neuroscience de Lyon, Centre Hospitalier Le Vinatier, Bâtiment 452, 95 Boulevard Pinel, 69500 Bron, France.

Tel.: +33 0 4 72 13 89 36.

** Corresponding author at: TIGER, Translational and Integrative Group in Epilepsy Research, INSERM U1028, CNRS UMR 5292, Centre de Recherche en Neuroscience de Lyon, CERMEP, 59 Bd Pinel, 69003, Lyon, France. Tel.: +33 0 4 72 357117.

E-mail addresses: carolina.ciumas@inserm.fr (C. Ciumas), ryvlin@cermep.fr (P. Ryvlin).

icEEG/fMRI;
Epilepsy;
RF heating

Methods: A human-shaped torso phantom and MRI-compatible intracerebral electrodes approved for icEEG in humans were used to mimic a patient with four intracerebral electrodes (one parasagittal and three coronal). Six rabbits were implanted with one or two coronal electrodes. MRI-induced temperature changes at the tip of electrodes were measured using a fibre-optic thermometer. All experiments were performed on Siemens Sonata 1.5 T scanner.

Results: For coronally implanted electrodes with wires pulled posteriorly to the magnetic bore, temperature increase recorded during EPI sequences reached a maximum of 0.6 °C and 0.9 °C in phantom and animals, respectively. These maximal figures were decreased to 0.2 °C and 0.5 °C, when electrode wires were connected to cables and amplifier. When electrode wires were pulled anteriorly to the magnetic bore, temperature increased up to 1.3 °C in both phantom and animals. Greater temperature increases were recorded for the single electrode implanted parasagittally in the phantom.

Conclusion: Variation of the temperature depends on the electrode and wire position relative to the transmit body coil and orientation of the constant magnetic field (B_0). EPI sequence with intracerebral electrodes appears as safe as standard T1 and T2 sequence for implanted electrodes placed perpendicular to the z-axis of the magnetic bore, using a 1.5 T MRI system, with the free-end wires moving posteriorly, in phantom and animals.

© 2013 Elsevier B.V. All rights reserved.

Introduction

Intracerebral electroencephalography (icEEG) recordings are used in patients suffering from drug-resistant partial epilepsy to determine the brain region generating seizures, and to plan the surgical resection that can free the patient from seizures. This is particularly useful in cases where non-invasive methods fail to precisely identify the so-called epileptogenic zone; a region of primary organization of seizures (Bancaud et al., 1965). icEEG allows capturing ictal discharges, interictal spikes, as well as bursts of pathological high frequency oscillations (HFOs), now considered the most reliable interictal indicator of the epileptogenic zone (Bragin et al., 2002). While icEEG proves successful in identifying the epileptogenic zone in a majority of cases (Guenot et al., 2001, 1999; Isnard et al., 1998; Khalfa et al., 2001; Ostrowsky et al., 2000; Ryvlin et al., 2006), its limited spatial sampling represents a major drawback. Regardless of the number of implanted electrodes, which commonly varies between centres and patients, less than 1% of the total brain volume is being recorded (Lachaux et al., 2003). Due to this spatial sampling limitation, the brain distribution of HFOs cannot be precisely ascertained using icEEG, while the possibility to detect and model HFOs using scalp EEG recordings remains a matter of debate. One way to address this issue would be to perform simultaneous acquisition of icEEG and fMRI data, with the aim of mapping blood oxygen level dependent (BOLD) signal changes associated with HFOs. fMRI offers whole-brain coverage at a quite good spatial and temporal resolution. Providing that interictal HFOs generate a detectable BOLD response (LeVan et al., 2010; Thornton et al., 2010), the latter would provide information about their distribution over the entire brain, including volume not sampled by icEEG. However, this approach raises the issue of MR safety and compatibility of medical devices. The presence of metallic conductors, more specifically the intracerebral electrodes, may be responsible for different hazards during MRI investigations, including (a) magnetically induced torque, (b) magnetically induced displacement forces, (c) induced currents generated by switching of magnetic field gradients, (d) gradient-induced vibration, and

(e) RF induced heating. Whereas all the above hazards are important and should be taken into account while using implanted electrodes (Carmichael et al., 2007; Georgi et al., 2004; Lemieux et al., 1997), most reports suggest that the highest safety risk factor is RF-induced heating (Carmichael et al., 2008; Georgi et al., 2004). The RF interaction with implants is complex and multi-parameter dependent. The implant's electric conductivity as well as dimensions and permittivity have to be considered, along with geometric arrangement relative to the specific MR coil and the properties of the MR sequence (Schaefers, 2008; Schaefers and Melzer, 2006). The American Society of Testing and Materials (ASTM) developed standards that are used to test for RF heating. It advises the use of fibre optic thermometer and a phantom filled with polyacrylic acid gel (Schaefers, 2008). It is also useful to determine in vivo temperatures in animals to ensure human safety. The in vivo temperatures in heated tissues strongly depend on blood perfusion, which redistributes RF heating (Baker et al., 2006). Several factors that might influence RF-induced heating associated with intracerebral electrodes need to be assessed, including the presence of closed loops of the implanted external wires, device position, MR system and sequences used, and specific absorption rate (SAR), in total the relative alignment to the electromagnetic field components.

Despite the above issues, structural MRI is commonly used in clinical practice (Wang et al., 2005) based on the approval of titanium MR conditional depth electrodes and reassuring clinical data (Pollo et al., 2003; Uitti et al., 2002; Vayssiere et al., 2000).

Conversely, echo planar imaging (EPI) sequences might carry different risks for RF power deposition. Recent studies in the field, limited to a phantom and a handful of patients, suggest that this is not the case (Boucoussis et al., 2012; Carmichael et al., 2008, 2010; Vulliemoz et al., 2010). To further investigate this issue, we performed a series of tests in a phantom and in animals implanted with the same depth electrodes as those used in patients with epilepsy, coupled with thermoprobes to precisely measure sequence-specific RF heating. We also systematically investigated the impact

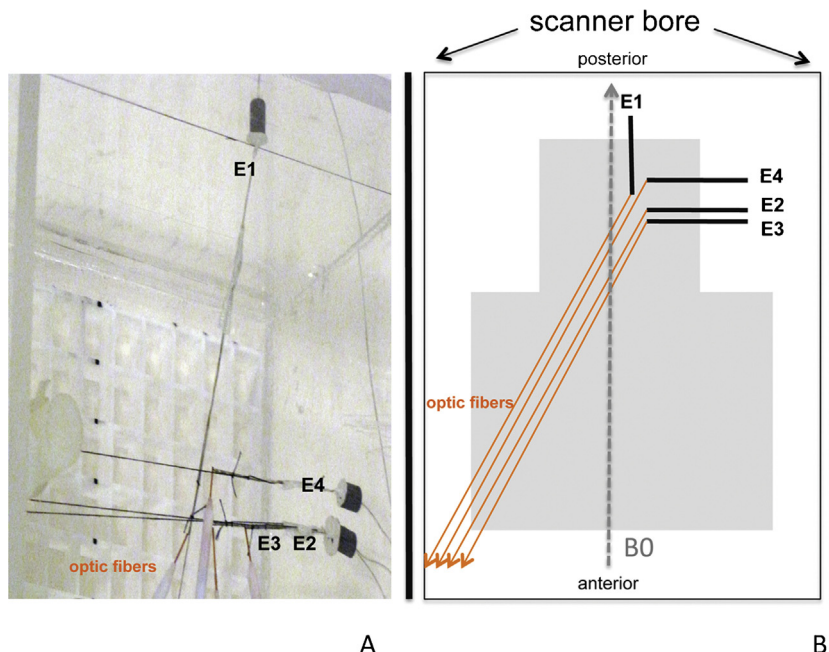


Figure 1 Experimental setup in the phantom. (A) A photograph of the phantom prepared for scanning. E3 is under E2 and is hardly detectable in the picture. (B) Schematic illustration of the experimental setup. Optic fibres were pulled outside the MR system and the temperature measurements were observed online during the scan. The free ends of the electrode wires were aligned either to the posterior or to the anterior end of the magnetic bore. E1 is placed parallel to the magnetic field (B_0) and to the z-axis. E2–E4 are perpendicular to this axis.

of positioning and connections of the electrodes, wires and cables, on the spatial distribution of RF energy deposition.

Materials and methods

All experiments were performed in a tissue-simulating phantom and in rabbits. The study was approved by the animal experimentation ethic committee of the University Claude Bernard Lyon I (Permit number: BH2009-26).

Phantom

We used an ASTM F2182-09 (ASTM, 2010) human-shaped torso phantom (MR:comp, Germany, Fig. 1), filled to a depth of about 15 cm with polyacrylic acid gel (10 g/L polyacrylic acid, 1.32 g/L NaCl and deionised water) to resemble human soft tissue permittivity and conductivity (0.47 S/m). The RF field and image intensity distributions of the phantom are optimal as its electrical properties and image intensity distribution is similar to the RF field distributions in human tissue at high fields (Wang et al., 2002).

Animals

All procedures were carried out with approval of the Animal Care Committee of Claude Bernard University (Lyon, France), in compliance with all local guidelines. Six adult female New Zealand white rabbits (Harlan, Gannat, France) weighing 2.7–3.2 kg were used in this study. They were housed in a room maintained at a constant temperature

of $21 \pm 1^\circ\text{C}$ and in a 12:12 h light–dark cycle with light onset at 6 A.M. Drinking water and food were provided ad libitum.

Electrodes

Standard, semiflexible platinum/iridium 5-contacts MR conditional depth electrodes (DIXI, Alcis, Besançon, France; diameter = 0.8 mm, contact length = 2 mm, intercontact interval = 1.5 mm, 100 mm in length) were used. These electrodes are the same as those used in patients in clinical practice (Catenoix et al., 2004; Ryvlin et al., 2006), and have been classified as MR-conditional for MRI environment from 1.5 to 3 T according to the ASTM classification (ASTM F2503-05). The electrodes were tested for induced torque (ASTM F2213-06), induced displacement (ASTM F2052-06c1), induced heating (ASTM 2182-02a) and deemed safe on all of the above.

Thermic probes for the phantom

Absolute temperature measurements were collected using a fibre optic thermometer (FOTEMP, Optocon) widely used in MRI RF safety measurements (Angelone et al., 2006; Baker et al., 2004). Temperature probes were placed at the tip of the electrode, which is believed to be the most RF sensitive location of the electrode (Pictet et al., 2002) (Fig. 1) and fixed with polyester strings.

Experimental settings in the phantom

The phantom was registered supine, head first, and the geometric centre of the head section was positioned at the isocentre of the scanner bore. Acrylic posts and pegboards were used to stabilize the active electrodes in position for each configuration during heating experiments. Each electrode was securely fastened so that it did not move during the experiments, and its wire remained in its free position to allow displacement during different experimental settings (reproducing clinical MRI investigation). Four holes were drilled in order to insert three coronal electrodes, including two electrodes at 1 cm distance from each other (E2 and E3) and another at 3 cm distance (E4), and one sagittal electrode (E1) perpendicular to E2–4 (Fig. 1). In clinical terms, the four electrodes were placed as follows: coronal – two on the left mimicking amygdala and hippocampus positioning (1 cm spacing) (E2 and E3), one electrode imitating the left insular positioning (E4), and one electrode on the perpendicular axis-the sagittal electrode (E1) (Fig. 1). The phantom was then assembled and kept at MR room temperature over 18 h. The temperature of the gel was stable at 20 °C (room temperature).

The free end of the electrode wire was used to loop the wire, to connect the wire to the cable, and to move it anterior or posterior to the magnetic bore. During runs that required cable connection, the wire was moved along the bore in the anterior-posterior direction to replicate the desired registration setting of an icEEG/fMRI experiment. The experiments on the phantom were conducted over a 2-day period. Each run was followed by a cooling period, typically in the range of 5–7 min, to allow the gel to return to baseline temperature, preventing subsequent measurement errors.

Thermic probes for *in vivo*

In vivo temperature measurements were performed using Luxtron (Luxtron 3204, Luxtron Corporation, Northwestern Parkway, CA, USA). The sensor was mounted adjacent to the electrodes with Teflon rubber.

Experimental settings in animals

The *in vivo* experiments were conducted six times on separate days. On the day of the experiment, surgery was performed under general anaesthesia to insert the intracranial electrode.

Rabbits were anaesthetized with a mixture of Ketamine hydrochloride (0.5 mL/kg) and Xylazine hydrochloride (50 mg/kg) injected intramuscularly, with additional intravenous (ear vein) Ketamine (67 mg) and Xylazine (33 mg). The latter was injected using a press-syringe at the speed of 0.03–0.08 mL/min, resulting in a flow of 1.8–4.8 mL/h adjusted to the cardiac rhythm, to ensure a proper level of anaesthesia during the whole experiment.

A skin incision between the right eye and ear was made, exposing the skull. The periost was subsequently removed, and a small burr hole was made. A titanium screw was placed in the burr hole, providing a fixed point for the electrode and the thermoprobe. All electrodes were inserted

coronally, in the temporal lobe. The extracranial part of the electrode was left underneath the screw. The animals were subsequently scanned in the prone position. Postoperative MRI was performed immediately after the implantation of the electrode. Similarly as in the phantom, we kept a pause between runs (around 5 min) until we achieved a stable temperature baseline, which took around 1.5–2 min.

There was no surgical or postoperative complication in all five rabbits where a single electrode was implanted. The sixth rabbit was implanted with two electrodes and developed intracerebral haemorrhage before the MRI scanning (MRI and postmortem examination of the brain) leading to its premature death just before the end of the experiment. Body temperature was controlled and maintained by warm blankets. The baseline temperature in rabbits was 38.5 °C on average and kept steady all along the experiment. At the end of the experiment, all animals were euthanized by an overdose (200 mg/kg) of Dolethal injected in the ear vein.

Since anaesthesia can cause linear temperature decay in animals (Shrivastava et al., 2008), the baseline temperature before each sequence was considered for calculation. Temperature was recorded continuously, with a sampling rate that varied between one measure every 1 or 3 s depending on the experiment. RF heating was calculated by subtracting the baseline temperature from the net temperature response measured at the tip of the electrode during the MR sequence.

MR imaging

All MRI experiments were performed using a Siemens Sonata whole-body 1.5 T MRI System (Siemens, Erlangen, Germany) associated to receive head coils (CP head coil for the phantom and 8-channel coil for rabbits) and transmit whole body coil. Several functional and structural sequences were performed, with the same imaging parameters for the phantom and animal studies.

Structural MRI

We used standard T1 and T2 FLAIR sequences similar to sequences used in patients undergoing icEEG to verify electrode placements. We also used a heating sequence (True fast imaging with steady precession [True-FISP]), with the purpose of obtaining effective thermal heating of the volume of interest (tissue surrounding the electrode) immediately before and after each sequence, to ensure that the thermoprobe was operating correctly. The scanning parameters for the T1 True-FISP sequence were: 192 × 192 matrix, TE = 1.82 ms, TR = 3.64 ms, FOV (in-plane) = 220 mm, flip angle = 60°, voxel size = 1.1 mm × 1.1 mm × 10 mm. Total scan time was 2.6 s. For the T1-weighted 3D sequence the parameters were: sagittal orientation, 160 slices, TE = 3.55 ms, TR = 2400 ms, TI = 1000 ms, FOV (in-plane) = 230 mm, flip angle = 8°, slice thickness = 1.2 mm, voxel size = 1.2 mm × 1.2 mm × 1.2 mm. Total scan time was 7 min 42 sec. The T2-weighted FLAIR sequence was acquired in coronal orientation, 120 slices, TE = 3.54 ms, TR = 5800 ms, TI = 2200 ms, FOV (in-plane) = 326 mm, slice thickness = 1.7 mm, voxel size = 1.7 mm × 1.7 mm × 1.7 mm. Total scan time was 5 min 22 s. T1- and T2-weighted FLAIR were used only in animals.

Functional MRI

We used the standard echo-planar imaging (EPI-FID) sequences performed in our centre in patients with epilepsy for mapping language and memory functions (64×64 matrix, TE = 50 ms, TR = 2500 ms, FOV (in-plane) = 220 mm, flip angle = 90°, 29 slices, 0.4 mm gap between, slice thickness = 3 mm, voxel size = 3.4 mm × 3.4 mm × 3.0 mm). 3, 6 and 10 minutes runs were performed.

Experimental procedures

Several conditions detailed below were investigated with respect to their impact on RF heating; (1) electrode position, (2) proximity of electrodes, (3) wire position, (4) creation of bundles, (5) cable connection, (6) amplifier connection, and (7) duration of EPI sequence. The axis of the electrode was perpendicular to the magnetic field direction for all but one phantom electrode where it was parallel to the z-axis. The impact of the proximity of electrodes on RF heating was tested by closely placing two electrodes in the phantom (E2 and E3, see Fig. 1), and by inserting two electrodes in one rabbit. The electrodes' free end wires were placed parallel to the magnetic bore, either anteriorly (in the direction of patients feet), or posteriorly (in the opposite direction). These wires were either separated from each other or bundled together at the exit from the phantom or from the animal's skull. The wires were either kept unconnected or connected to non-ferromagnetic cables (260 cm) approved for scalp-EEG/fMRI experiments in humans. The latter were placed in the same direction than the wires (i.e. either moving anteriorly or posteriorly within the magnetic bore), and were connected or not to an fMRI dedicated compatible 64-channel EEG amplifier (MICROMED, Italy).

Statistical analysis

We used a Mann–Whitney nonparametric test to compare temperature changes detected under the different conditions.

Results

Temperature measurement

All configurations and corresponding highest changes in temperature (ΔT_s) are summarized in Table 1. Each True-FISP sequence resulted in brief spikes of increased temperature ranging from 0.4 to 0.8 °C, which quickly recovered. The duration of EPI sequence had no influence on the recorded variations in temperature, in line with the fact that the latter always peaked within the first minute following onset of scanning (Fig. 2).

Phantom experiments

Using the standard coronal position of intracerebral electrodes used in patients with epilepsy, the elevation of the temperature during an EPI sequence varied from 0 to 1.3 °C. However, temperature changes significantly differ as a function of the anterior or posterior position

of the wires free ends in the magnetic bore ($p=0.001$). When placed posteriorly, temperature varied from 0 to 0.6 °C (mean \pm SD = 0.2 \pm 0.2 °C), versus 0.3 to 1.3 °C (mean \pm SD = 0.7 \pm 0.4 °C) when placed anteriorly. There was a non-significant trend towards lower temperature values when the wires were connected to the cables and the amplifier. Bundling the wires did not have any impact on temperature, neither the duration of the EPI sequence, or the proximity of electrodes E2 and E3, as compared to E4.

In contrast with coronal electrodes, that placed sagittally (E1) was associated with raised temperature when not connected, regardless of the anterior (0.6–2.2 °C) or posterior (0.1–4.9 °C) position of the wire in the magnetic bore, Fig. 2. Conversely, any configuration with this electrode wire connected to the cable and the amplifier resulted in modest temperature changes (0.1–0.6 °C), except when it formed buckles with other electrodes' wires (1.8 °C).

Animal experiments

The structural MRI sequences resulted in temperature variations of 0.1–1 °C for the 3D T1, and 0.4–1.3 °C for the T2 FLAIR. Similarly, EPI sequences were associated with ΔT_s of 0–1.3 °C. As for phantom experiment, ΔT_s significantly differ as a function of the direction of the free end wire within the magnetic bore ($p=0.003$). When the free end wires were pulled posteriorly, ΔT_s ranged from 0.1 to 0.9 °C (mean \pm SD = 0.5 \pm 0.2 °C), while it varied between 0 and 1.3 °C (mean \pm SD = 0.8 \pm 0.4 °C) when placed anteriorly. There was no significant impact of any other parameters, including connection to cables and amplifier, bundling of wires, duration of EPI sequence, or and presence of two electrodes in rabbit 6.

Discussion

We investigated RF power deposition during MRI, and especially during EPI sequence acquisition, under varying experimental conditions, to better understand the relative risk of RF-induced heating of the tissue that surrounds intracerebral electrodes. Our study is the first that has evaluated temperature change during functional and structural MRI in animals with implanted electrodes, thus accounting for perfusion in the brain and associated heat dispersion (Baker et al., 2006). Based on our findings, it appears that EPI sequence with intracerebral electrodes can be considered as safe as standard T1/T2 anatomical sequences for implanted electrodes placed perpendicular to the z-axis of the magnetic bore, using a 1.5 T MRI system, with the free-end wires moving posteriorly. In patients undergoing intracerebral EEG recording, this would correspond to electrodes inserted in the coronal plane using a so-called "orthogonal approach". Connection to cables and amplifier, which is expected to be used during fMRI experiments in patients undergoing icEEG recordings, does not seem to significantly influence RF-induced heating in phantom and animals.

Our measurement followed an amended ASTM based testing procedure for RF heating of passive implants at a time where the comprehensive approach provided in ISO/TS 10974 (issued May 2012) for active implantable medical

Table 1 Variation of the temperature during EPI scanning.

	EPI		
	Phantom		Rabbits
	Perpendicular electrode position, average ΔT_s (min–max)	Parallel electrode position, average ΔT_s (min–max)	Parallel electrode position, average ΔT_s (min–max)
Wires are pulled in the back, parallel to B_0			
Electrodes wires not connected to the cable	2.5 (0.2–4.9)	0.2 (0–0.6)	0.4 (0.1–0.9)
Electrodes wires not connected to the cable, wires in buckles	0.1 (0.1–0.2)	0.2 (0.1–0.5)	0.4 (0.1–0.7)
Electrodes wires not connected to the cable, long sequence (6–10 min)	0.2 (0.2)	0.3 (0.1–0.5)	0.7 (0.6–0.8)
Electrodes wires connected to the cable	0.2 (0.2)	0.3 (0.1–0.4)	0.5 (0.2–0.8)
Electrodes wires connected to the cable, wires in buckles			0.3 (0.3)*‡
Electrodes wires connected to the cable, long sequence	0.1 (0–0.1)	0.1 (0.1–0.2)	0.5 (0.4–0.6)
Electrodes wires connected to the cable, wires are separated, connected to the amplifier	0.1 (0.1)	0.1 (0.1)	0.5 (0.5)*‡
Electrodes wires connected to the cable, wires in buckles, connected to the amplifier	1.8 (1.8)*	0.2 (0.1–0.2)	0.4 (0.4–0.5)
Wires are aligned in the front, parallel to B_0			
Electrodes wires not connected to the cable	1.4 (0.6–2.2)	1 (0.6–1.3)	1.1 (0.8–1.3)
Electrodes wires not connected to the cable, wires in buckles	0.7 (0.7)	1 (0.6–1.3)	0.6 (0.1–1.1)
Electrodes wires connected to the cable	0.6 (0.6)	0.5 (0.3–0.6)	0.1 (0–0.2)
Electrodes wires connected to the cable, wires in buckles			0.7 (0.1–1.2)
Electrodes wires connected to the cable, long sequence (6–10 min)	0.5 (0.5)	0.5 (0.5)	0.2 (0.1–0.3)
Electrodes wires connected to the cable, wires are separated, connected to the amplifier	0.5 (0.5)	0.5 (0.5)	1 (1)*‡
Electrodes wires connected to the cable, wires in buckles, connected to the amplifier		0.5 (0.5)	

ΔT_s : temperature difference subtracted between pick of temperature elevation during a sequence and the baseline.

* Single value, experimental setting was not repeated.

‡ Only in the rabbit that was implanted with two electrodes. Values in parentheses represent the variation in ΔT_s : from lowest to highest; single value means repetitive registration of ΔT_s for the given experimental condition. Empty cases mean that for this experimental setting the temperature logfile was unusable or that it was not explored during the experiment.

devices such as pacemakers and neurostimulators with flexible electrodes was still under development. Thus, our experiments, which show only a part of the electrode case matrix, do not satisfy all current MR safety statements for scanning brain electrodes, even though it provides unique *in vivo* data. Furthermore, our experiments do not address the specific issues raised by other types of intracranial electrodes used in patients with refractory partial epilepsy, in particular the widely used subdural grids and strips. Finally, neither the small animal nor the human sized phantom can fully account for the exact electromagnetic field distribution found in the human head. In particular, the small size of the rabbit brain resulted in only one or two electrodes and temperature probes implanted in those animals. However, data obtained in rabbits as well as in phantom suggest

that the proximity of the two implanted electrodes, reflecting minimal distance between intracerebral electrodes used in patients with epilepsy, might not result in an increase in RF heating. In order to prove this, we would need to transfer experimental results to the human brain via numerical simulations. Another limitation is the number of animal experiments, which was compensated for by the high reproducibility of our findings.

While no comparable study has yet been performed in animals, our results are fully consistent with data obtained in previous phantom studies (Carmichael et al., 2008, 2010). Carmichael et al. performed such experiments with use of depth (3 electrodes; Carmichael et al., 2010), grid and strip electrodes, varying cable length (80–180 cm), cable placement (in the back and in the front as well as under the

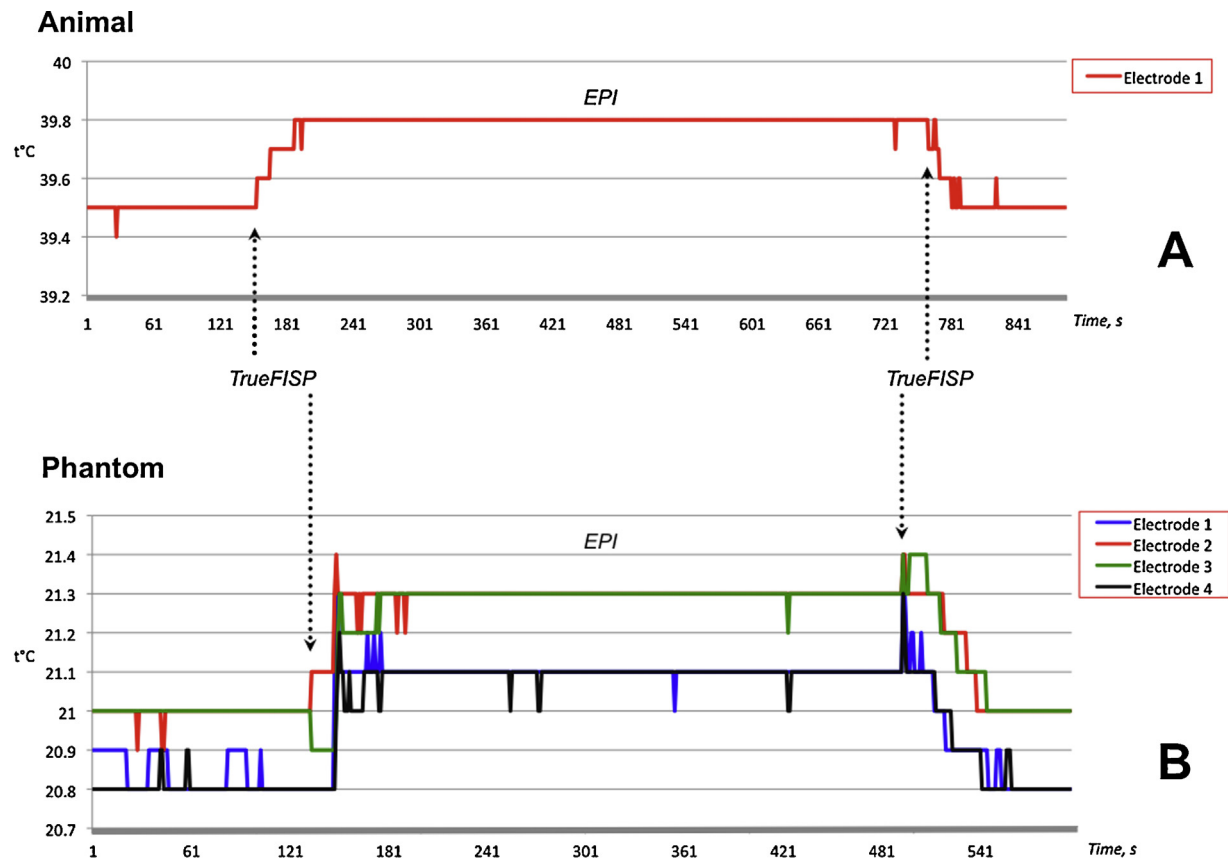


Figure 2 Temperature curves in the animal (A) and in the phantom (B) measured during the MRI acquisition. (A) is a 10 min recording in the rabbit and (B) is a 6 min recording in the phantom. The setup in A and B are identical, electrodes wires were not connected to the cable, and wires were pulled back and parallel to the B_0 field. Arrows indicate the variation of the temperature related to the onsets of TrueFISP sequences.

coil), connection to the amplifier (open and closed circuits), coils (head or body transmit coils) and field strength (1.5 T Siemens Avanto and 3 T Siemens Trio and 3 T GE Signa scanners). In accordance with our own findings, they reported no increase above 1 °C using 1.5 T Siemens EPI acquisitions. The similarity between their observations and our data are compelling, given that we did not use the exact same scanner (1.5 T Siemens Sonata), coils (head receive coil), cables (260 cm), MR sequences (slightly different parameters for the EPI sequence), nor the same thermometry methods.

The only situations where we observed increased temperature above 1 °C was when using sagittal electrodes placed parallel to the z-axis in phantom, and when the free-end wires of the electrodes moved anteriorly within the magnetic bore in both phantom and rabbits. The latter situation was also tested in phantom by Carmichael et al. (2010), showing greater heating than when the free-end wires were moved posteriorly, though not exceeding 1 °C when using 1.5 T scanner. Conversely, sagittal depths electrodes were not tested in their study where other parameters could be associated with significant heating (3 T, position of the electrode towards the B_0 axis). Overall, it appears that EPI sequence in patients with intracerebral electrodes should be restricted to patients where all electrodes are implanted in the coronal plane using an orthogonal approach (thus placed perpendicular to the z-axis of the magnetic bore), using a

1.5 T MRI system, with the free-end wires moving posteriorly. Connection to cables and amplifier, which is expected to be used during fMRI experiments in patients undergoing icEEG recordings, does not seem to significantly influence RF-induced heating.

Interestingly, we observed moderate increases of the temperature during T1- and T2-weighted FLAIR sequences in rabbits, up to 1.3 °C, thus comparable to those measured during EPI acquisition. For these experiments, we used the same MRI sequences and MR conditional electrodes that are routinely used in a large number of epilepsy surgery centres. No complication of such investigations has been so far reported in humans, suggesting that the maximal 1.3 °C RF-induced heating observed in our animals might still reflect a safe procedure, even though it is usually recommended to ensure RF-induced heating lower than 1 °C. Similarly, the first attempts to perform combined icEEG and fMRI in humans, at either 1.5 T (Carmichael et al., 2012; Vulliemoz et al., 2010) or 3 T (Cunningham et al., 2012), was not associated with any detectable complication.

In vitro studies have demonstrated that the specific absorption rate (SAR) of the MRI scan correlates with the temperature increase at the tip of the electrode (Rezai et al., 2002). Our EPI sequence RF exposure was restricted to 0.1 W/kg, which is within the guidelines. While higher SAR could be a potential safety hazard, no complication was

observed in 211 deep brain stimulation patients that underwent one, two or three post-implantation MRI investigations, including 34 diffusion weighted imaging acquisitions with 0.8 and 0.9 W/kg SAR (Weise et al., 2010).

Overall, and despite the lack of comprehensive testing according to the recently released ASTM guidelines, the bulk of data obtained to date suggest that provided the specific safety constraints discussed above, RF heating associated with EPI sequences acquired in patients with intracerebral electrodes might be qualitatively similar to that associated with the standard T1 and T2 imaging routinely used in those patients to precisely locate the position of the electrodes.

Conflict of interest

None of the authors has any conflict of interest to disclose.

Acknowledgements

We thank MR:comp (Germany), DIXI (France), and MicroMed (France) for their kind support of phantom and animal experiments. We are very grateful to Christian Koch for recording temperature. We also thank Valerie Detti useful discussion about our experimental setup.

References

- Angelone, L.M., Varios, C.E., Wiggins, G., Purdon, P.L., Bonmassar, G., 2006. On the effect of resistive EEG electrodes and leads during 7 T MRI: simulation and temperature measurement studies. *Magn. Reson. Imaging* 24 (6), 801–812.
- ASTM, F2182-09, 2010. Standard Test Method for Measurement of Radio Frequency Induced Heating Near Passive Implants During Magnetic Resonance Imaging.
- Baker, K.B., Tkach, J.A., Nyenhuis, J.A., Phillips, M., Shellok, F.G., Gonzalez-Martinez, J., et al., 2004. Evaluation of specific absorption rate as a dosimeter of MRI-related implant heating. *J. Magn. Reson. Imaging* 20 (2), 315–320.
- Baker, K.B., Tkach, J.A., Phillips, M.D., Rezai, A.R., 2006. Variability in RF-induced heating of a deep brain stimulation implant across MR systems. *J. Magn. Reson. Imaging* 24 (6), 1236–1242.
- Bancaud, J., Talairach, J., Bonis, A., Schaub, C., 1965. La stereoelectroencephalographie dans l'épilepsie: informations neurophysiopathologiques apportées par l'investigation fonctionnelle stereotaxique. Paris.
- Boucoussis, S.M., Beers, C.A., Cunningham, C.J., Gaxiola-Valdez, I., Pittman, D.J., Goodyear, B.G., et al., 2012. Feasibility of an intracranial EEG-fMRI protocol at 3 T: risk assessment and image quality. *Neuroimage* 63 (3), 1237–1248.
- Bragin, A., Mody, I., Wilson, C.L., Engel Jr., J., 2002. Local generation of fast ripples in epileptic brain. *J. Neurosci.* 22 (5), 2012–2021.
- Carmichael, D.W., Pinto, S., Limousin-Dowsey, P., Thobois, S., Allen, P.J., Lemieux, L., et al., 2007. Functional MRI with active, fully implanted, deep brain stimulation systems: safety and experimental confounds. *Neuroimage* 37 (2), 508–517.
- Carmichael, D.W., Thornton, J.S., Rodionov, R., Thornton, R., McEvoy, A., Allen, P.J., et al., 2008. Safety of localizing epilepsy monitoring intracranial electroencephalograph electrodes using MRI: radiofrequency-induced heating. *J. Magn. Reson. Imaging* 28 (5), 1233–1244.
- Carmichael, D.W., Thornton, J.S., Rodionov, R., Thornton, R., McEvoy, A.W., Ordidge, R.J., et al., 2010. Feasibility of simultaneous intracranial EEG-fMRI in humans: a safety study. *Neuroimage* 49 (1), 379–390.
- Carmichael, D.W., Vulliemoz, S., Rodionov, R., Thornton, J.S., McEvoy, A.W., Lemieux, L., 2012. Simultaneous intracranial EEG-fMRI in humans: data quality. *Neuroimage*.
- Catenoix, H., Guenot, M., Isnard, J., Fischer, C., Mauguire, F., Ryvlin, P., 2004. Intracranial EEG study of seizure-associated nose wiping. *Neurology* 63 (6), 1127–1129.
- Cunningham, C.B.J., Goodear, B.G., Badawy, R., Zaamout, F., Pittman, D.J., Beers, C.A., et al., 2012. Intracranial EEG-fMRI analysis of focal epileptiform discharges in humans. *Epilepsia*, 1–13.
- Georgi, J.C., Stippich, C., Tronnier, V.M., Heiland, S., 2004. Active deep brain stimulation during MRI: a feasibility study. *Magn. Reson. Med.* 51 (2), 380–388.
- Guenot, M., Isnard, J., Ryvlin, P., Fischer, C., Ostrowsky, K., Mauguire, F., et al., 2001. Neurophysiological monitoring for epilepsy surgery: the Talairach SEEG method. StereoElectroEncephaloGraphy. Indications, results, complications and therapeutic applications in a series of 100 consecutive cases. *Stereotact. Funct. Neurosurg.* 77 (1-4), 29–32.
- Guenot, M., Krolak-Salmon, P., Mertens, P., Isnard, J., Ryvlin, P., Fischer, C., et al., 1999. MRI assessment of the anatomy of optic radiations after temporal lobe epilepsy surgery. *Stereotact. Funct. Neurosurg.* 73 (1–4), 84–87.
- Isnard, J., Guenot, M., Fischer, C., Mertens, P., Sindou, M., Mauguire, F., 1998. A stereoelectroencephalographic (SEEG) study of light-induced mesiotemporal epileptic seizures. *Epilepsia* 39 (10), 1098–1103.
- Khalfa, S., Bougeard, R., Morand, N., Veillet, E., Isnard, J., Guenot, M., et al., 2001. Evidence of peripheral auditory activity modulation by the auditory cortex in humans. *Neuroscience* 104 (2), 347–358.
- Lachaux, J.P., Rudrauf, D., Kahane, P., 2003. Intracranial EEG and human brain mapping. *J. Physiol. Paris* 97 (4–6), 613–628.
- Lemieux, L., Allen, P.J., Franconi, F., Symms, M.R., Fish, D.R., 1997. Recording of EEG during fMRI experiments: patient safety. *Magn. Reson. Med.* 38 (6), 943–952.
- LeVan, P., Tyvaert, L., Moeller, F., Gotman, J., 2010. Independent component analysis reveals dynamic ictal BOLD responses in EEG-fMRI data from focal epilepsy patients. *Neuroimage* 49 (1), 366–378.
- Ostrowsky, K., Isnard, J., Ryvlin, P., Guenot, M., Fischer, C., Mauguire, F., 2000. Functional mapping of the insular cortex: clinical implication in temporal lobe epilepsy. *Epilepsia* 41 (6), 681–686.
- Pictet, J., Meuli, R., Wicky, S., van der Klink, J.J., 2002. Radiofrequency heating effects around resonant lengths of wire in MRI. *Phys. Med. Biol.* 47 (16), 2973–2985.
- Pollo, C., Meuli, R., Maeder, P., Vingerhoets, F., Ghika, J., Villemure, J.G., 2003. Subthalamic nucleus deep brain stimulation for Parkinson's disease: magnetic resonance imaging targeting using visible anatomical landmarks. *Stereotact. Funct. Neurosurg.* 80 (1-4), 76–81.
- Rezai, A.R., Finelli, D., Nyenhuis, J.A., Hrdlicka, G., Tkach, J., Sharpen, A., et al., 2002. Neurostimulation systems for deep brain stimulation: in vitro evaluation of magnetic resonance imaging-related heating at 1.5 tesla. *J. Magn. Reson. Imaging* 15 (3), 241–250.
- Ryvlin, P., Minotti, L., Demarquay, G., Hirsch, E., Arzimanoglou, A., Hoffman, D., et al., 2006. Nocturnal hypermotor seizures, suggesting frontal lobe epilepsy, can originate in the insula. *Epilepsia* 47 (4), 755–765.
- Schaefers, G., 2008. Testing MR safety and compatibility: an overview of the methods and current standards. *IEEE Eng. Med. Biol.* 27 (3), 23–27.

- Schaefers, G., Melzer, A., 2006. Testing methods for MR safety and compatibility of medical devices. *Minim. Invasive Ther. Allied Technol.* 15 (2), 71–75.
- Shrivastava, D., Hanson, T., Schlentz, R., Gallagher, W., Snyder, C., Delabarre, L., et al., 2008. Radiofrequency heating at 9.4 T: in vivo temperature measurement results in swine. *Magn. Reson. Med.* 59 (1), 73–78.
- Thornton, R.C., Rodionov, R., Laufs, H., Vulliemoz, S., Vaudano, A., Carmichael, D., et al., 2010. Imaging haemodynamic changes related to seizures: comparison of EEG-based general linear model, independent component analysis of fMRI and intracranial EEG. *Neuroimage* 53 (1), 196–205.
- Uitti, R.J., Tsuboi, Y., Pooley, R.A., Putzke, J.D., Turk, M.F., Wszolek, Z.K., et al., 2002. Magnetic resonance imaging and deep brain stimulation. *Neurosurgery* 51 (6), 1423–1428, discussion 1428–1431.
- Vayssiere, N., Hemm, S., Zanca, M., Picot, M.C., Bonafe, A., Cif, L., et al., 2000. Magnetic resonance imaging stereotactic target localization for deep brain stimulation in dystonic children. *J. Neurosurg.* 93 (5), 784–790.
- Vulliemoz, S., Carmichael, D.W., Rosenkranz, K., Diehl, B., Rodionov, R., Walker, M.C., et al., 2010. Simultaneous intracranial EEG and fMRI of interictal epileptic discharges in humans. *Neuroimage* 54 (1), 182–190.
- Wang, J., Yang, Q.X., Zhang, X., Collins, C.M., Smith, M.B., Zhu, X.H., et al., 2002. Polarization of the RF field in a human head at high field: a study with a quadrature surface coil at 7.0T. *Magn. Reson. Med.* 48 (2), 362–369.
- Wang, Y., Agarwal, R., Nguyen, D., Domocos, V., Gotman, J., 2005. Intracranial electrode visualization in invasive pre-surgical evaluation for epilepsy. In: Conf Proc IEEE Eng Med Biol Soc 1, pp. 952–955.
- Weise, L.M., Schneider, G.H., Kupsch, A., Haumesser, J., Hoffmann, K.T., 2010. Postoperative MRI examinations in patients treated by deep brain stimulation using a non-standard protocol. *Acta Neurochir. (Wien)* 152 (12), 2021–2027.